Journal of Cleaner Production 234 (2019) 810–821

Contents lists available at ScienceDirect

Journal of Cleaner Production

journal homepage: www.elsevier.com/locate/jclepro

Modeling and optimal scheduling of battery energy storage systems in electric power distribution networks

Hasan Mehrjerdi [a], Reza Hemmati [b, *]

[a] Electrical Engineering Department, Qatar University, Doha, Qatar
[b] Department of Electrical Engineering, Kermanshah University of Technology, Kermanshah, Iran

ARTICLE INFO

Article history:
Received 17 September 2018
Received in revised form
15 November 2018
Accepted 17 June 2019
Available online 25 June 2019

Handling Editor: Cecilia Maria Villas Bôas de Almeida

Keywords:
Battery energy storage system (BESS)
Capability curve
Mixed integer linear programming (MILP)
Distribution network
Operation optimization

ABSTRACT

Thanks to the unique features, deployment of battery energy storage systems in distribution systems is ever-increased. Therefore, new models are needed to capture the real-life characteristics. Beside active power, the battery energy storage system can exchange reactive power with the grid due to the inverter-based connection. Although some previous works have considered this issue, a detailed linear model suitable for the realistic large scale distribution systems is not addressed adequately. In this context, this paper proposes a mixed integer linear programming model for optimal battery energy storage system operation in distribution networks. The proposed model considers various parts of the battery energy storage system including battery pack, inverter, and transformer in addition to linear modeling of the reactive power and apparent power flow limit. Moreover, a linear power flow model is used to calculate voltage magnitudes and power losses with high accuracy. The proposed model is applied to the IEEE 33-bus test case and the results prove the accuracy and efficiency of the proposed model. The results demonstrate that considering reactive capability of the batteries offers new benefits including voltage profile improvement, decreasing reactive power flow in the network, reducing network losses, and releasing network and substation capacity.

1. Introduction

Nowadays, Energy Storage Systems (ESSs) are not new devices in the power systems. The emergence of these devices in the power systems was the deployment of the pumped hydro units for load leveling in Europe. Subsequently, development of the renewable power resources and need for smoothing generated power magnified role of the ESSs. In this stage, various ESS technologies including pumped hydro units, compressed air energy storage (CAES), thermal storage, hydrogen storage (along with fuel cell), flywheels, supercapacitor, superconducting magnetic energy storage (SMES) and various battery technologies have been utilized to renewable energy integration and time shift (Whittingham, 2012). With introducing smart grid concepts, the ESSs attract more attentions owing to the numerous and unique applications besides renewable energy assistant including price arbitrage (Saboori and Hemmati, 2016), peak shaving (Pimm et al., 2018), loss reduction (Saboori and Abdi, 2013), supply capacity, spinning reserve, load following, area regulation, transmission and distribution upgrade deferral (Kleinberg et al., 2014), congestion management (Hemmati et al., 2017), reactive support and power quality (Mahela and Abdul, 2016), reliability (Awad et al., 2014), and black start and restoration (Liu et al., 2016).

Among various ESS technologies, Battery Energy Storage Systems (BESS) are becoming prominent technology for almost all applications owing to the unique feature including (Lawder et al., 2014).

1. Modular system
2. Quiet operation
3. Minimum environmental manipulation
4. Non-polluting parts
5. Possibility to achieve a wide range of technical features
6. Quick and compact installation
7. Relatively fast response time
8. High power and energy density
9. High efficiency

* Corresponding author. Department of Electrical Engineering, Kermanshah University of Technology, Iran, Kermanshah, P.O.Box: 67156-85420, Iran.
E-mail addresses: Hasan.mehrjerdi@qu.edu.qa (H. Mehrjerdi), r.hemmati@kut.ac.ir (R. Hemmati).

https://doi.org/10.1016/j.jclepro.2019.06.195
0959-6526/

Nomenclature

Sets

Ω_K	Time periods
Ω_N	Generating units
Ω_B	Network buses
Ω_S	Battery energy Storage systems (BESSs)
Ω_Y	Auxiliary variable for linearization
Ω_{NB}	Generating units installed in the bus n
Ω_{SB}	BESSs installed in the bus n

Parameters

$P_n^{\min}$	Lower limit of active power generation of unit n (kW)
$P_n^{\max}$	Upper limit of active power generation of unit n (kW)
$\Delta P_{n,k,p}^{gen}$	Slope of segment p of generation cost function of unit n at time period k ($/kW)
$Q_n^{\min}$	Lower limit of reactive power generation of unit n (kVaR)
$Q_n^{\max}$	Upper limit of reactive power generation of unit n (kVaR)
$C_g^{\min}$	Generation cost at minimum power output on unit n ($)
$C_{b,k}^{LL}$	Cost of load shedding at bus b and time period k ($/kW)
$PD_{b,k}$	Active power demand at bus b and time period k (kW)
$QD_{b,k}$	Reactive power demand at bus b and time period k (kVaR)
$G_{b,bb}^{L}$	Line conductance between buses b and bb (mho)
$B_{b,bb}^{L}$	Line susceptance between buses b and bb (mho)
E_s^0	Initial energy stored in BESS s (kWh)
η^C	BESSs charging efficiency
η^D	BESS discharging efficiency
EB_s^{rated}	Energy capacity rating of BESS s (kWh)
SB_s^{rated}	Power rating of BESS s (kVA)

Variables

OC_{Tot}	Total daily operation cost ($)
$C_{n,k}^{gen}$	Generation cost of unit n at time period k ($)
$C_{b,k}^{shed}$	Load shedding cost of bus b at time period k ($)
$\Delta C_{n,k,p}^{gen}$	Auxiliary variable of segment p of generation cost function of unit n at time period k (kW)
$PG_{n,k}$	Active power generated by unit n at time period k (kW)
$QG_{n,k}$	Reactive power generated by unit n at time period k (kVaR)
$PL_{b,k}$	Active power shed in bus b and time period k (kW)
$QL_{b,k}$	Reactive power shed in bus b and time period k (kVaR)
$PB_{s,k}^{C}$	Active charging power of BESS s at time period k (kW)
$PB_{s,k}^{D}$	Active discharging power of BESS s at time period k (kW)
$QB_{s,k}^{C}$	Reactive charging power of BESS s at time period k (kVaR)
$QB_{s,k}^{D}$	Reactive discharging power of BESS s at time period k (kVaR)
$PF_{b,bb,k}$	Active power flow between buses b and bb at time period k (kW)
$QF_{b,bb,k}$	Reactive power flow between buses b and bb at time period k (kVaR)
$E_{s,k}$	Energy stored in BESS s at time period k (kWh)
$IP_{s,k}^{C}$	Binary variable indicating active charging power status of BESS s at time period k
$IP_{s,k}^{D}$	Binary variable indicating active discharging power status of BESS s at time period k
$IQ_{s,k}^{C}$	Binary variable indicating reactive charging power status of BESS s at time period k
$IQ_{s,k}^{D}$	Binary variable indicating reactive discharging power status of BESS s at time period k
$PB_{s,k}^{sqr}$	Auxiliary variable indicating square of net active power exchange of BESS s at time period k
$QB_{s,k}^{sqr}$	Auxiliary variable indicating square of net reactive power exchange of BESS s at time period k
$V_{b,k}^{sqr}$	Square of voltage magnitude of bus b at time period k (PU)
$\theta_{b,k}^{bus}$	Voltage angle of bus b at time period k (rad)

Nowadays, various BESSs are developed and commercialized to use in the power systems. Considering range of the power and energy, the BESSs are employed mainly in the distribution systems (Saboori et al., 2017).

Various research papers have been worked on the modeling and operation of the ESS in general and the BESS particularly. In Hemmati and Saboori (2016) a general model is proposed for ESS contribution in unit commitment along with sensitivity analysis. The model is a Direct Current (DC) one and does not consider reactive power of the network and the ESS. The results show that taking ESS into account in the unit commitment model will decrease operation cost as a function of the ESS power rating and energy capacity. In Saboori and Hemmati (2017) the ESS reactive contribution along with the distributed generation resources are considered with a non-linear model solved by heuristics algorithms. The proposed model is used to enhance distribution company (DISCO) profit by benefiting from price arbitrage. The authors have proposed an unbalance three-phase BESS scheduling and operation system for 4-wire low voltage distribution grids in Bennett et al. (2015); Watson et al. (2018); Sabillon-Antunez et al. (2017). In these works, either the reactive power is not take into account or the model is non-linear. In Bennett et al. (2015) the three-phase model us used to balance system currents where load leveling is the primary application of the BESS. As stated by the authors, their proposed model has been able to achieve defined goals including load leveling and system balancing. In Watson et al. (2018) the authors have been focused on proposing a non-linear but convex model for distribution system operation with storage devices. The simulation results in Sabillon-Antunez et al. (2017) demonstrate that electric vehicle charging is performed coordinately taking into account Volt-VAr control, energy storage device and dispatchable distributed generation resources installed in three-phase unbalanced distribution networks. Theoretic simulations and realistic experiments are performed in Reihani et al. (2016) for optimal charging and discharging of batteries in order to peak shaving, load curve smoothing, and voltage control. Although the reactive power of the BESS is considered that is not aimed directly in the objective function in addition to the fact that the proposed model is non-linear. Their results have been show that the BESS operation does not have significant impact on the feeder voltage but can be used to serve the reactive loads on the circuit and reduce the reactive loads of the system.

In Hosseina and Taghi Bathaee (2016) operation of the redox flow BESS is addressed in the distribution networks with the aim of peak shaving and load leveling. The proposed method does not address reactive power capability. Optimal operation of the distribution grid equipped with dispersed generation resources and BESS via a Multi-Objective Energy Management (MOEM) is addressed in Azizivahed et al. (2018). The reactive power is modeled with non-linear equations and thud a heuristic algorithm, namely, Hybrid Grey Wolf Optimizer-Particle Swarm Optimization (HGWO-PSO) is used. The authors in Grillo et al. (2012) have been proposed a model for the optimal operation of a hot-temperature (sodium nickel chloride) BESS connected with wind turbines in a medium voltage distribution system. While the proposed model has been confirmed via experimental tests, the reactive power is not focused.

Inverter-based operation of the BESS offers flexibility in absorbing or injecting active and/or reactive power. But, this should be modeled accurately to capture its applicability. Although some researches consider reactive flow in the networks many of them don't take into account BESS contribution in reactive power. Even with considering BESS reactive power, proposed works are not linear and are solved using evolutionary algorithms or BESS reactive capability is not modeled based on the capability curve. In this regard, this paper aims to model BESS accurately by considering various constituent parts including battery pack, inverter, and transformer in addition to the reactive power contribution based on the capability curve. The proposed model takes the advantage of BESS's inverter reactive power exchange with the grid in time periods with no or little active power exchange leading to auxiliary benefit of voltage regulation besides conventional load leveling. The proposed model is a Mixed Integer Linear Programming (MILP), suitable for realistic very large scale distribution networks, robustness in terms of convergence to the global optima, easily solvable by commercial solvers in addition to the calculating voltage magnitudes and network losses with precise linear equations. To demonstrate the usability of the model, is tested on the IEEE 33 bus distribution test system and the results are presented and discussed. The results demonstrated that not considering BESS reactive capability leads to underestimate its benefits for the grid operator. The contribution of the paper can be listed briefly as follows.

- Modeling BESS considering constituting parts including battery pack, conversion unit, and transformer.
- Modeling BESS reactive power contribution based on the 4-quadratnt capability curve.
- Mixed Integer Linear Programming (MILP) model for optimal BESS operation.
- Evaluating effects of considering BESS reactive contribution on the obtained benefits.

The remainder of the paper is organized as follows. The proposed model including BESS, network model, and operation optimization is presented in section II. Section III demonstrates the test case, inputs, results, and analysis. Afterwards, section IV draw some conclusions and remarks for the summarization.

2. Proposed model

In this section, the proposed formulation will be described in details which is a Mixed Integer Linear Program (MILP). The MILP is a form of the linear programs in which some variables are required to take integer values. In other word, in the MILP model, objective function and all constraints are linear but some variables may be integers while some others are continuous. The term “Mixed” in the acronym denotes a mixture of the continuous and integer variables. These optimization models arise naturally in many problems and possess diverse applications in various engineering fields. The MILP benefits from the linear structure of the problem including efficiently solvable by strong commercial solvers and guaranteed convergence to the global optima. The integer variables usually come from the nature of the problem. In the proposed model, integer variables are used to control BESS status between charging and discharging actions. Explanation of the proposed method is performed in three step, namely:

A. Objective function
B. BESS model
C. Power flow

2.1. Objective function

Objective function of the problem is tailored so as to take into account two cost terms, namely power generation cost and load shedding cots. Power generation cost is associated with cost of providing electric energy from the network generators and/or upstream substation. In addition, shedding costumer load will impose a cost on the system operator. The generation cost is function of the consumed power and related cost factor. Load shedding cost is related to the amount of the shed load and also value of the lost load. As presented in (1), generation cost and load shedding cost are elaborated over all generating units and network buses at all constituting time periods, respectively.

$$OC_{Tot} = \sum_{n,\,k} C^{gen}_{n,\,k} + \sum_{b,\,k} C^{shed}_{b,\,k} \tag{1}$$

To keep linear nature of the problem, a piecewise linearization technique is used to convert original quadratic generation cost function. This is a well-known and trusted approximation method and detailed explanations about this method is presented in the Appendix (Hemmati and Saboori, 2017). Substituting equations are presented in (2) to (5).

$$C^{gen}_{n,\,k} = C^{\min}_{g} + \sum_{p} \Delta C^{gen}_{n,k,p}\ \Delta P^{gen}_{n,k,p} \quad \forall\ n \in \Omega_N\ ,\ \forall\ k \in \Omega_K \backslash \tag{2}$$

$$PG_{n,k} = \sum_{p} \Delta P^{gen}_{n,k,p} + P^{\min}_{n} \quad \forall\ n \in \Omega_N\ ,\ \forall\ k \in \Omega_K \tag{3}$$

$$Q^{\min}_{n} \le QG_{n,k} \le Q^{\max}_{n} \quad \forall\ n \in \Omega_N\ ,\ \forall\ k \in \Omega_K \tag{4}$$

$$P^{\min}_{n} \le PG_{n,k} \le P^{\max}_{n} \quad \forall\ n \in \Omega_N\ ,\ \forall\ k \in \Omega_K \tag{5}$$

Shedding load by the operator will result in monetary payment to the costumers with respect to the bus location, time periods, and amount of lost load. This cost component is formulated in (6) to (8). In (6) the cost of load shedding is calculated as a linear function of shed power and Value of Lost Load (VOLL). Equation (7) declares that the shed power at each bus and time period should be a positive value lower than the bus demand. This mean that load shedding cannot act as a generation resource and is limited to the reduction of the bus demand to no-load situation. In (8) it is indicated that by shedding bus active demand, the reactive demand is also curtailed with the same ratio.

$$C^{shed}_{b,\,k} = C^{LL}_{b,\,k}\ PL_{b,\,k} \quad \forall\ b \in \Omega_B\ ,\ \forall\ k \in \Omega_K \tag{6}$$

$$0 \le PL_{b,\,k} \le PD_{b,k} \;\forall\; b \in \Omega_B \,,\; \forall\; k \in \Omega_K \tag{7}$$

$$QL_{b,\,k} = \frac{PL_{b,\,k}}{PD_{b,k}} QD_{b,k} \;\;\forall\; b \in \Omega_B \,,\; \forall\; k \in \Omega_K \tag{8}$$

2.2. BESS model

An Energy Storage System (ESS) can store energy at time periods with low demand and then release the stored storage at time periods with high demand. This energy consumption time shift, or equivalently energy arbitrage or load leveling, brings many benefits to the system operation. Obtained benefits are a direct result of the shaving the peak profile. The first and foremost benefit of the energy arbitrage is total electric energy production (purchase) cost reduction. The energy cost reduction is based on the fact that cost of providing electric power is a second order function of the produced power. Therefore, providing energy needed in the peak periods where energy cost is high at time periods with low demand where energy cost is low causes significant cost different. Energy arbitrage offers some by-products including power losses, voltage drop, and emissions reduction in addition to the releasing network capacity. Various methods have been developed in order to store electric energy in a ESS including:

1. Pumped hydro energy storage
2. Compressed air energy storage
3. Hydrogen storage in addition to fuel cell
4. Flywheel energy storage
5. Supercapacitor energy storage
6. Superconducting magnetic energy storage (SMES)
7. Electrochemical battery energy storage

Among the abovementioned ESS technologies only Battery Energy Storage System (BESS) have been developed and matured to use in distribution network. The reason is that some ESS technologies, i.e. pumped hydro and compressed air energy storage, requires special land or geographic formations which they cannot easily found anywhere. Also, some other are in the experimental stage and commercial production requires high investment expenses namely SMES. Storing hydrogen as a medium and releasing back by means of fuel cell have a low round trip efficiency. Other remained ESS technologies including supercapacitor, flywheel, and SMES have very low discharge time and cannot be used in the energy management applications like energy arbitrage.

Among various ESS technologies, Battery Energy Storage Systems (BESS) are becoming prominent technology for almost all applications owing to the unique feature including (Lawder et al., 2014).

1. Modular system
2. Quiet operation
3. Minimum environmental manipulation
4. Non-polluting parts
5. Possibility to achieve a wide range of technical features
6. Quick and compact installation
7. Relatively fast response time
8. High power and energy density
9. High efficiency

The key factors to exploit functionalities of the BESS are precise modeling and optimal scheduling in the system. To do this, we first present the model of the BESS and then optimize the proposed model in a daily operation scheduling problem. General function of the BESS in the system when it is connected to a bus is presented in Fig. 1. The figure illustrates the bus (node) view point of the BESS system. From the bus view, the BESS acts as a load at charging mode and a generator at discharging mode. Consequently, the role of the BESS in the power flow of the system can be reflected in the bus power balance equations for both active and reactive powers. To do this, charging power of the BESS regarded as a fictitious demand and therefore will be added to the consumption side of the bus power balance equation for both active and reactive powers. Similarly, discharging power of the BESS should be added to the generation side of the bus power balance equation as a new generation source. Equations (9) and (10) give the mathematical expressions of the above statement for active and reactive power balances, respectively. As the equations show, charging power of the BESSs, bus demand, and summation over all flows sent to the connected lines belong to the power consumption side of the equations. In the contrary, discharging power of the all BESSs, generated power by the installed generating units and up-stream substation, and shed load are considered as generation side of the equations.

$$\sum_{s \in \Omega_{SB}} PB^{C}_{s,k} + PD_{b,k} + \sum_{bb} PF_{b,bb,k} = \sum_{n \in \Omega_{NB}} PG_{n,k} + \sum_{s \in \Omega_{SB}} PB^{D}_{s,k} + PL_{b,k} \;\forall\; b, bb \in \Omega_B \,,\; \forall\; k \in \Omega_K \tag{9}$$

$$\sum_{s \in \Omega_{SB}} QB^{C}_{s,k} + QD_{b,k} + \sum_{bb} QF_{b,bb,k} = \sum_{n \in \Omega_{NB}} QG_{n,k} + \sum_{s \in \Omega_{SB}} QB^{D}_{s,k} + QL_{b,k} \;\forall\; b, bb \in \Omega_B \,,\; \forall\; k \in \Omega_K \tag{10}$$

As it is illustrated in Fig. 1, the incoming power into the BESS and also the outgoing power from the BESS are exposed to the charging and discharging units limitations and characteristics. It should be noted that the BESS starts the daily operation process with an initial and predefined stored energy level, as it is shown in (11). The stored energy in the BESS at any time period is a function of the stored energy, charged power, and discharged power at the previous time period. Equation (12) demonstrates this situation and declares that

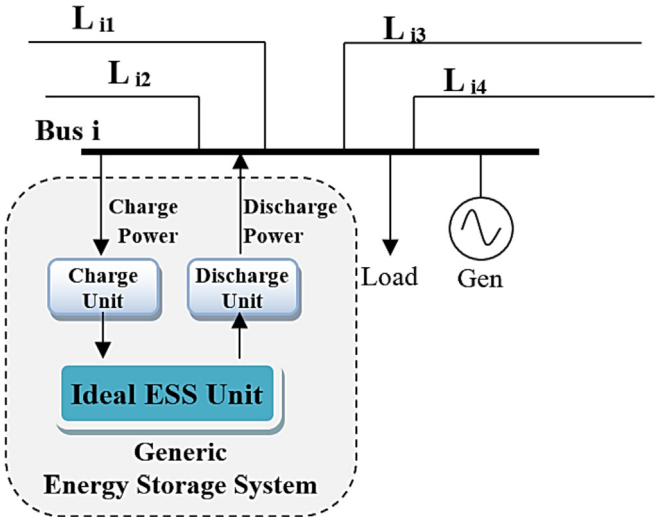

Fig. 1. Bus impact of the BESS.

some of the drawn power from the grid to charge and also some of the released power form the BESS at discharge mode will be lost owing to the charging and discharging units internal losses. The stored energy in the BESS cannot exceeds its rated energy capacity. The inequalities in (13) ensure that the stored energy of the BESS is a positive value limited to the rated energy capacity. Also, at the end of the time periods, stored energy in the BESS should be equal to the initial value as it is shown by (14).

$$E_{s,k} = E_s^0 \quad \forall \ s \in \Omega_S \ , \ k = 1 \tag{11}$$

$$E_{s,k} = E_s^0 + \sum_{kk=1}^{k-1} PB_{s,kk}^C \eta^C - \sum_{kk=1}^{k-1} PB_{s,kk}^D \Big/ \eta^D \quad \forall \quad s \in \Omega_S \ , \ k \in \Omega_K \tag{12}$$

$$0 \le E_{s,k} \le \ EB_s^{rated} \quad \forall \quad s \in \Omega_S \ , \ k \in \Omega_K \tag{13}$$

$$\sum_{k=1}^{K} PB_{s,k}^C \eta^C = \sum_{k=1}^{K} PB_{s,k}^D \Big/ \eta^D \tag{14}$$

Fig. 2 shows that the whole BESS system is composed of three parts. The main part of the system is battery pack. The battery pack is composed of battery modules wherein each battery module is a set of battery cells. The battery pack is responsible for storing and delivering electric energy but with Direct Current (DC) waveform. Considering that the grid is constructed and operated with Alternating Current (AC) waveform, a converting device is needed. This conversion will be performed in the Power Conversion Unit (PCU). The PCU converts AC power of the grid to the DC charging power needed in charging mode of the battery pack. In the contrary, it converts DC delivered power of battery pack to the AC power of the grid in the discharging mode of the battery pack. Considering that AC output voltage of the PCU is limited to the low voltage range, a step-up transformer is needed to enhance inverted AC voltage to the grid voltage of the connection bus.

The BESS can choose one of the actions charging mode, discharging mode, or doing nothing at any time period. Strictly speaking, charging and discharging modes cannot take place simultaneously. This is the case for the both active and reactive powers. To establish such a situation, a binary variable is used which switching its value between zero and unity changes the BESS charging/discharging mode. Equation (15) states this matter mathematically for the active power exchange. In addition, active charging and discharging powers should be less than the BESS apparent power after switching corresponding binary value to unity, as declared in (16) and (17). This situation is also hold for the reactive power, namely binary switching and apparent power limitation. Equations (18)–(20) are equivalent constraints for the reactive power same as the active power. Finally, a BESS at any time period cannot inject power to the grid more that its stored energy multiplied by the discharging efficiency. Equation (21) represents this constraint on the BESS discharging power.

$$IP_{s,k}^C + IP_{s,k}^D \le 1 \quad \forall \quad s \in \Omega_S \ , \ k \in \Omega_K \tag{15}$$

$$PB_{s,k}^C \le IP_{s,k}^C \ SB_s^{rated} \ \forall \quad s \in \Omega_S \ , \ k \in \Omega_K \tag{16}$$

$$PB_{s,k}^D \le IP_{s,k}^D \ SB_s^{rated} \ \forall \quad s \in \Omega_S \ , \ k \in \Omega_K \tag{17}$$

$$IQ_{s,k}^C + IQ_{s,k}^D \le 1 \quad \forall \quad s \in \Omega_S \ , \ k \in \Omega_K \tag{18}$$

$$QB_{s,k}^C \le IQ_{s,k}^C \ SB_s^{rated} \ \forall \quad s \in \Omega_S \ , \ k \in \Omega_K \tag{19}$$

$$QB_{s,k}^D \le QP_{s,k}^D \ SB_s^{rated} \ \forall \quad s \in \Omega_S \ , \ k \in \Omega_K \tag{20}$$

$$PB_{s,k}^D \le E_{s,k} \eta_{dis}^D \quad \forall \quad s \in \Omega_S \ , \ k \in \Omega_K \tag{21}$$

At last but not the least, apparent power flow of the BESS should be confined to the rated apparent power defined by the conversion system and the used transformer. The BESS apparent power flow is a non-linear function of the exchanged active and reactive power, as mathematically expressed in (22).

$$\sqrt{P^2 + Q^2} \le S \tag{22}$$

There are two problems with this constraint. The first is that one variable is defined for each of the active and reactive powers while the BESS uses two for each of them, i.e., charging and discharging. Considering this fact that at any time period only one of the charging and discharging powers have a value greater than zero, net active power exchange can be defined as the summation of the charging and discharging powers. This situation is a direct result of equation (15). This is also the case for the reactive power considering (18). By substituting this terms in (22), the flow limit can be expressed as (23).

$$\sqrt{\left(PB_{s,k}^C + PB_{s,k}^D\right)^2 + \left(QB_{s,k}^C + QB_{s,k}^D\right)^2} \le SB_s^{rated} \quad \forall \ s \in \Omega_S \ , \ k \in \Omega_K, \ y \in \Omega_Y \tag{23}$$

The second problem is with the non-linearity. This is addressed here by approximating second order terms with piecewise linear terms. As declare in (24) and (25) second order functions of the active and reactive powers are replaced with corresponding new linear functions. By substituting new linear functions in the (23), one can calculate (26) and the root square can be easily removed as in (27) considering that BESS rated apparent power is a constant value.

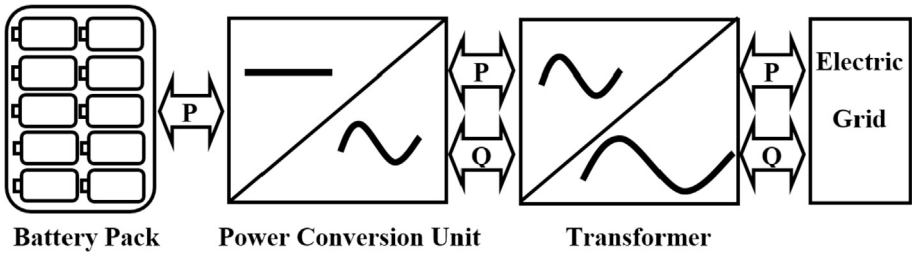

Fig. 2. The BESS constituting parts.

$$\left(PB^{C}_{s,k}+PB^{D}_{s,k}\right)^{2} = PB^{sqr}_{s,k} \quad s\in\Omega_S,\ k\in\Omega_K,\ y\in\Omega_Y \tag{24}$$

$$\left(QB^{C}_{s,k}+QB^{D}_{s,k}\right)^{2} = QB^{sqr}_{s,k} \quad s\in\Omega_S,\ k\in\Omega_K,\ y\in\Omega_Y \tag{25}$$

$$\sqrt{PB^{sqr}_{s,k}+QB^{sqr}_{s,k}} \le SB^{rated}_{s} \quad \forall\ s\in\Omega_S,\ k\in\Omega_K,\ y\in\Omega_Y \tag{26}$$

$$PB^{sqr}_{s,k}+QB^{sqr}_{s,k} \le \left(SB^{rated}_{s}\right)^{2} \quad \forall\ s\in\Omega_S,\ k\in\Omega_K,\ y\in\Omega_Y \tag{27}$$

Only remained task is defining linearized term for the square of the active and reactive powers. These are implemented in (28) and (29) by using piecewise linearization (Explained in Appendix) for active and reactive powers in turn. By substituting (28) and (29) in (27) the final linear constraint for the apparent power flow of the BESS can be expressed as (30) instead original non-linear one in (22).

$$PB^{sqr}_{s,k} = \sum_{y}\left[(2y+1)\times\left(\frac{SB^{rated}_{s}}{Y}\right)\Delta P^{BES}_{s,y,k}\right] \quad \forall\ s\in\Omega_S,\ k\in\Omega_K,\ y\in\Omega_Y \tag{28}$$

$$QB^{sqr}_{s,k} = \sum_{q}\left[(2y+1)\left(\frac{SB^{rated}_{s}}{Y}\right)\Delta Q^{BES}_{s,y,k}\right] \quad \forall\ s\in\Omega_S,\ k\in\Omega_K \tag{29}$$

$$\sum_{y}\left[(2y+1)\left(\frac{SB^{rated}_{s}}{Y}\right)\left(\Delta P^{BES}_{s,y,k}+\Delta Q^{BES}_{s,y,k}\right)\times\right] \le \left(SB^{rated}_{s}\right)^{2} \quad \forall\ s\in\Omega_S,\ k\in\Omega_K,\ y\in\Omega_Y \tag{30}$$

At last, some supporting equations are needed to define limit and slope of each piece line of the linearized equivalent which are defined in (31) to (34) and (35) to (38) for active and reactive power, respectively.

$$\sum_{y}\Delta P^{BES}_{s,y,k} = PB^{C}_{s,k}+PB^{D}_{s,k} \quad \forall\ s\in\Omega_S,\ k\in\Omega_K,\ y\in\Omega_Y \tag{31}$$

$$0 \le \Delta P^{BES}_{s,y,k} \le \frac{SB^{rated}_{s}}{Y} \quad \forall\ s\in\Omega_S,\ k\in\Omega_K,\ y\in\Omega_Y \tag{32}$$

$$\Delta P^{BES}_{s,y,k} \le \frac{SB^{rated}_{s}}{Y}\ \Delta PI_{s,y-1,k} \quad \forall\ s\in\Omega_S,\ k\in\Omega_K,\ y\in\Omega_Y \tag{33}$$

$$\frac{SB^{rated}_{s}}{Y}\ \Delta PI_{s,Y,k} \le \Delta P^{BES}_{s,y,k} \quad \forall\ s\in\Omega_S,\ k\in\Omega_K,\ y\in\Omega_Y \tag{34}$$

$$\sum_{y}\Delta Q^{BES}_{s,y,k} = QB^{C}_{s,k}+QB^{D}_{s,k} \quad \forall\ s\in\Omega_S,\ k\in\Omega_K,\ y\in\Omega_Y \tag{35}$$

$$0 \le \Delta Q^{BES}_{s,y,k} \le \frac{SB^{rated}_{s}}{Y} \quad \forall\ \forall\ s\in\Omega_S,\ k\in\Omega_K,\ y\in\Omega_Y \tag{36}$$

$$\Delta Q^{BES}_{s,y,k} \le \frac{SB^{rated}_{s}}{Y}\ \Delta QI_{s,y-1,k} \quad \forall\ s\in\Omega_S,\ k\in\Omega_K,\ y\in\Omega_Y \tag{37}$$

$$\frac{SB^{rated}_{s}}{Y}\ \Delta QI_{s,y,k} \le \Delta Q^{BES}_{s,y,k} \quad \forall\ s\in\Omega_S,\ k\in\Omega_K,\ y\in\Omega_Y \tag{38}$$

2.3. Power flow

For the power flow equations, a newly proposed and trusted method is used. The details of the model can be found in Zhang et al. (2013) and (Yuan et al., 2018) where its functionality is challenged in Yang et al. (2017). The active power flow considering voltage magnitudes of the buses is defined in (39) where the reactive power equivalent is presented in (40). The second term in (39) and (40) stands for half of the line loss. The non-linearity of the bus voltage angle in this terms can be easily removed by a method similar to the BESS flow limit, namely piecewise linearization.

$$PF_{b,bb,k} = G^{L}_{b,bb}\left(V^{sqr}_{b,k}-V^{sqr}_{bb,k}\right) - B^{L}_{b,bb}\left(\theta^{bus}_{b,k}-\theta^{bus}_{bb,k}\right) + G^{L}_{b,bb}\left(\frac{\left(\theta^{bus}_{b,k}-\theta^{bus}_{bb,k}\right)^{2}}{2}\right) \quad \forall\ b,bb\in\Omega_B,\ k\in\Omega_K \tag{39}$$

$$QF_{b,bb,k} = -B^{L}_{b,bb}\left(V^{sqr}_{b,k}-V^{sqr}_{bb,k}\right) - G^{L}_{b,bb}\left(\theta^{bus}_{b,k}-\theta^{bus}_{bb,k}\right) - B^{L}_{b,bb}\left(\frac{\left(\theta^{bus}_{b,k}-\theta^{bus}_{bb,k}\right)^{2}}{2}\right) \quad \forall\ b,bb\in\Omega_B,\ k\in\Omega_K \tag{40}$$

3. Case study

The model proposed in the previous section is implemented on the IEEE 33-bus distribution test system. This test system is a hypothetical medium voltage distribution network proposed by M. E. Baran and F. F. Wu in 1989 (Baran and Wu, 1989). This system has been recognized by the Institute of Electrical and Electronics Engineers (IEEE) as a benchmark for the electric power distribution network studies. The system has constituted a basis for simulation studies in distribution networks and is one the most popular test systems in the field. Fig. 3 shows the single line diagram of the system. It has one feeder with nominal voltage of 12.66 kV and with

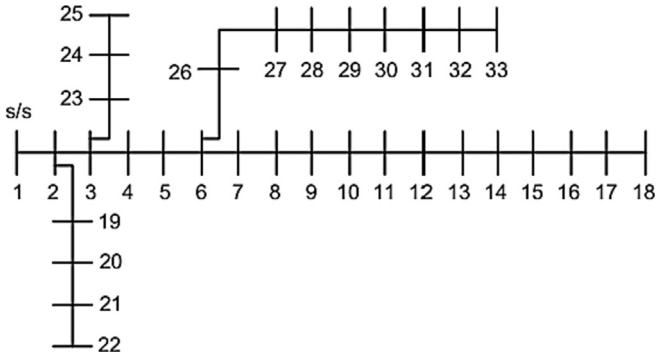

Fig. 3. Single line diagram of the IEEE 33-bus distribution test system.

four different laterals, 32 branches and a total peak load of 3715 kW and 2300 kVAr. Line and bus load data are presented in Table 1. It should be noted that bus 1 (substation) has no active and reactive load.

As in the original network, the network is supplied only with the up-stream substation. The only change is adding two identical BESSs (denoted by BESS 1 and BESS 2) in buses 18 and 33 each with 500 kVA power rating and 1500 kWh energy capacity. Also, a daily time horizon consists of 24 1-h time periods is considered. Hourly bus active and reactive load factors are presented in Table 2 (Grigg et al., 1999). For the sake of simplicity and without loss of generality, a step-wise power generation cost is considered wherein the cost is increased constantly for each 500 kWh. The generation cost factors are presented in Fig. 4 (Zhang et al., 2017). Voltage set point of the substation is regulated in 1.02 per-unit to compensate voltage drop in the feeders. The model is implemented in the GAMS (Brook and KendrickAlexander, 1988) environment and is solved using CPLEX (Cplex, 2007) solver.

In order to demonstrate applicability of the proposed method, three different cases are simulated. In Case 1, a conventional distribution network without BESS is considered. In Case 2, the proposed method is tested wherein the distribution network is installed with the BESSs and reactive power contribution is considered. Finally, Case 3 denotes a system with the BESSs but without reactive contribution. Table 3 shows the simulation results for the Case 1 and Case 2 in addition to the comparisons. The table shows total indices including total daily operation, daily cost difference in terms of dollars and percent, voltage index value and absolute and relatively difference. In addition, last rows represent total daily active and reactive power losses and their differences for the both cases.

Table 2
Hourly load factors [%].

Hour	**1**	**2**	**3**	**4**	**5**	**6**
Factor	67	63	60	59	59	60
Hour	**7**	**8**	**9**	**10**	**11**	**12**
Factor	74	86	95	96	96	95
Hour	**13**	**14**	**15**	**16**	**17**	**18**
Factor	95	95	93	94	99	100
Hour	**19**	**20**	**21**	**22**	**23**	**24**
Factor	100	96	91	83	73	63

As it is demonstrated by the results, total daily operation cost is reduced by 1190 dollars equal to 6.173 percent because of the optimal BESS scheduling. This cost reduction is a direct result of optimal load leveling by the BESSs. It should be noted that, load leveling by the BESSs offers some other advantages besides cost reduction including power loss reduction and voltage profile improvement.

Total active and reactive power losses of the network with and without BESS are presented in the table. These values are calculated as the difference between injected power to and drawn power from the feeder. The presented losses are summation over all time periods and show total daily energy loss in the network. As the results show, total daily losses for both active and reactive powers are decreased by approximately one fourth as a results of optimal BESS scheduling. The Voltage Index (VI) is calculated by summing up all of the bus voltage deviations from the unity and over all time periods, namely:

$$VI = \sum_{b,k} |1 - V_{b,k}| \tag{41}$$

Table 1
Line and load data of IEEE 33-bus distribution test system.

Line Location		Line Parameters		Bus Loads at Receiving Bus	
Sending Bus	Receiving Bus	R (Ω)	X (Ω)	P (kW)	Q (kVAr)
1	2	0.0922	0.047	100	60
2	3	0.493	0.2511	90	40
3	4	0.366	0.1864	120	80
4	5	0.3811	0.1941	60	30
5	6	0.819	0.707	60	20
6	7	0.1872	0.6188	200	100
7	8	0.7114	0.2351	200	100
8	9	1.03	0.74	60	20
9	10	1.044	0.74	60	20
10	11	0.1966	0.065	45	30
11	12	0.3744	0.1238	60	35
12	13	1.468	1.155	60	35
13	14	0.5416	0.7129	120	80
14	15	0.591	0.526	60	10
15	16	0.7463	0.545	60	20
16	17	1.289	1.721	60	20
17	18	0.732	0.574	90	40
2	19	0.164	0.1565	90	40
19	20	1.5042	1.3554	90	40
20	21	0.4095	0.4784	90	40
21	22	0.7089	0.9373	90	40
3	3	0.4512	0.3083	90	50
23	24	0.898	0.7091	420	200
24	25	0.896	0.7011	420	200
6	26	0.203	0.1034	60	25
26	27	0.2842	0.1447	60	25
27	28	1.059	0.9337	60	20
28	29	0.8042	0.7006	120	70
29	30	0.5075	0.2585	200	600
30	31	0.9744	0.963	150	70
31	32	0.3105	0.3619	210	100
32	33	0.341	0.5302	60	40

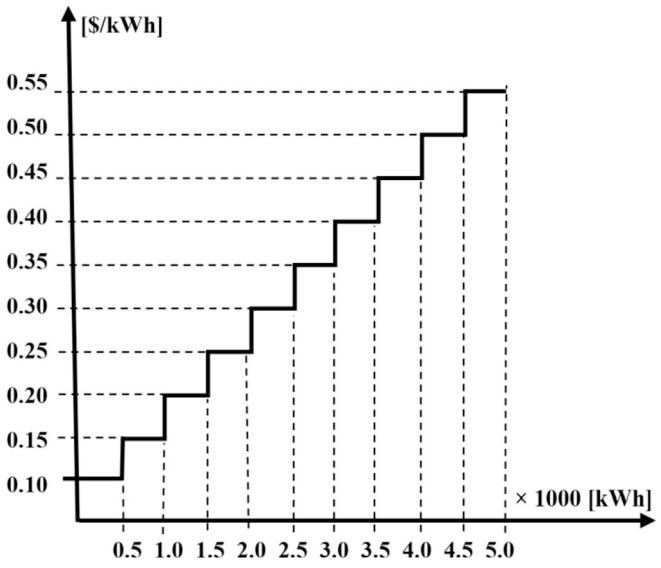

Fig. 4. Step-wise generation cost function (Zhang et al., 2017).

Table 3
Simulation results for Cases 1 and Case 2.

Total Operation Cost ($)	**Case 1**	**Case 2**
	20,474	19,284
Operation Cost Difference	**$**	**%**
	1,190	6.173
Voltage Index Value	**Case 1**	**Case 2**
	57.754	41.264
Voltage Index Difference	**VI**	**%**
	16.49	28.55
Active Power	**Case 1**	**Case 2**
Losses (kWh)	7349.676	5495.948
Active Losses Difference	**kWh**	**%**
	1853.728	25.22
Reactive Power Losses (kVArh)	**Case 1**	**Case 2**
	4834.904	3687.488
Reactive Losses Difference	**kVArh**	**%**
	1147.416	23.73

This index is a measure of voltage profile flatness and is calculated to demonstrate effect of the BESS reactive contribution on the network voltage profile. As indicated in the table, considering reactive power contribution of the BESS in the network, improves voltage of the buses significantly as the VI is decrease about one third.

Table 4 presents the simulation results but ignoring BESS

Table 4
Simulation results for Case 1 and Case 3.

Total Operation Cost ($)	**Case 1**	**Case 3**
	20,474	20,025
Operation Cost Difference	**$**	**%**
	449.362	2.244
Voltage Index Value	**Case 1**	**Case 3**
	57.754	57.562
Voltage Index Difference	**VI**	**%**
	0.192	0.33
Active Power	**Case 1**	**Case 3**
Losses (kWh)	7349.676	7221.919
Active Losses Difference	**kWh**	**%**
	127.75	1.73
Reactive Power Losses (kVArh)	**Case 1**	**Case 3**
	4834.904	4758.541
Reactive Losses Difference	**KVArh**	**%**
	76.36	1.57

Table 5
Simulation results for Case 2 and Case 3.

Total Operation Cost ($)	**Case 3**	**Case 2**
	20,025	19,284
Operation Cost Difference	**$**	**%**
	741	3.7
Voltage Index Value	**Case 3**	**Case 2**
	57.562	41.264
Voltage Index Difference	**VI**	**%**
	16.298	28.31
Active Power	**Case 3**	**Case 2**
Losses (kWh)	7221.919	5495.948
Active Losses Difference	**kWh**	**%**
	1725.971	23.90
Reactive Power Losses (KVArh)	**Case 3**	**Case 2**
	4758.541	3687.488
Reactive Losses Difference	**KVArh**	**%**
	1071.053	22.50

reactive power contribution. The Case 1 and Case 3 are compared based on the general simulation results. As the results show, neglecting BESS reactive capability results to less benefits of the BESS in terms of cost reduction, loss reduction, and voltage improvement compared to the Case 2. The reason for these results is that reactive power is flow only from the substation and causes active and reactive power losses in the network. Also, bus voltages are almost without change with respect to the case without BESS.

Table 5 contains simulation results for the Case 2 and Case 3 and magnifies benefits of the proposed model. As it is indicated by the results, taking BESS reactive contribution into account have a positive impact on the various economic and technical factors. Most important improvement is occurred in the total operation cost which it is improved by 3.7 percent. Also, modeling BESS reactive capability causes a 28.31 percent improvement in the voltage profile leading to a flatter curve. The largest effect of the BESS reactive power contribution is on the power losses. As the results shows, by calling BESS reactive power, power flow in the network will be decreased. Decreasing power flow will result to lessening network active/reactive losses, in turn.

Fig. 5 illustrates hourly generated power in the network including power to supply loads, network losses, and net exchange of the BESS in the case with them. This power is the output power of the up-stream substation supplying the network. As the figure shows, in the case without the BESS there is a considerable variation from off-peak to peak hours resulting to power production

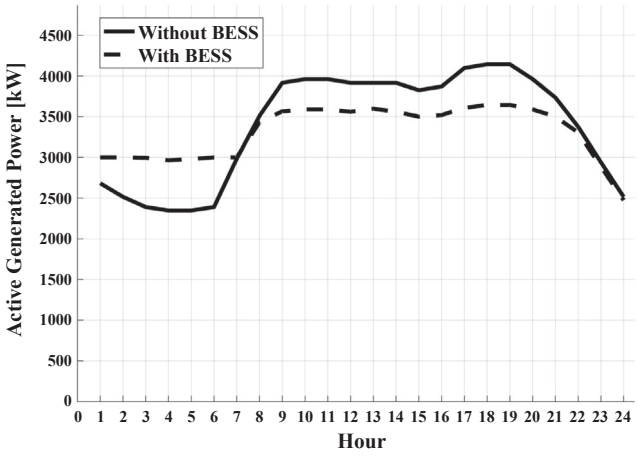

Fig. 5. Total hourly generated active power (substation output) with and without BESS 1 and BESS 2.

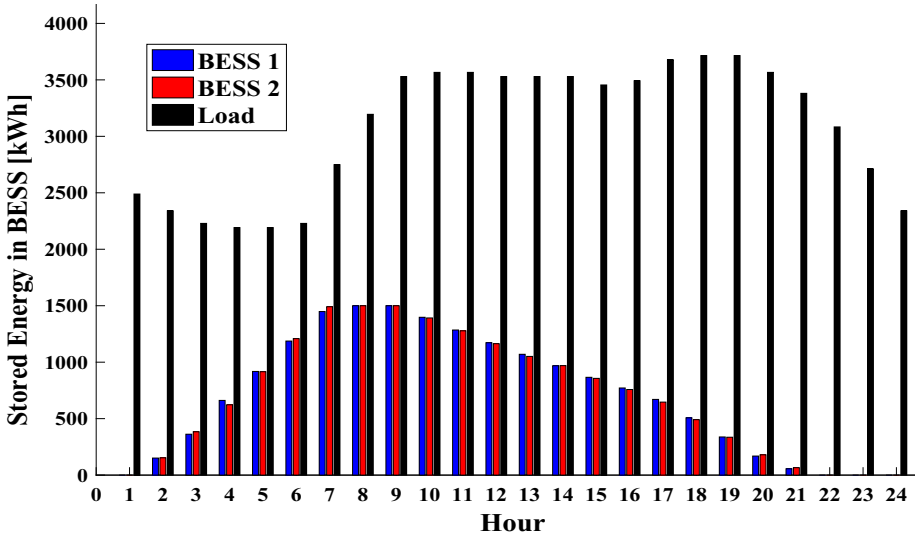

Fig. 6. Stored energy in BESS 1 and BESS 2 with respect to the active load.

cost. In the second case, the curve is flattened by optimal charging and discharging of the BESS. In fact, the valley is filled by the charging power to shave the peak by discharging stored power. Stored energy in the BESSs for each one and any hour in addition to the active load profile is depicted in Fig. 6. The figure conveys two deductions. The first is that the trend of accumulating energy in the BESSs is quite in accordance with the load profile, i.e., using off-peak hours to store energy as much as possible and deliver stored energy in the peak periods. The second deduction is that both of the BESSs respect their predefined energy capacity limit. Furthermore, Table 6 represents hourly charging and discharging powers for both BESSs in which absorb power at the time periods with low generation cost and inject it at the time periods with the time periods with the high generation cost.

Total network active power losses for each time period is shown

Table 6
Hourly active load and charging and discharging power for BESS 1 and BESS 2.

Hour	Active Load	Active Charging		Active Discharging	
		BESS 1	BESS 2	BESS 1	BESS 2
1	2489	150	153	0	0
2	2340	211	230	0	0
3	2229	299	238	0	0
4	2191	256	292	0	0
5	2191	269	292	0	0
6	2229	261	282	0	0
7	2749	51	8	0	0
8	3194	0	0	0	0
9	3529	0	0	102	108
10	3566	0	0	112	114
11	3566	0	0	112	114
12	3529	0	0	102	112
13	3529	0	0	101	81
14	3529	0	0	102	112
15	3454	0	0	94	98
16	3492	0	0	101	111
17	3677	0	0	163	155
18	3715	0	0	169	155
19	3715	0	0	169	155
20	3566	0	0	112	114
21	3380	0	0	56	65
22	3083	0	0	0	0
23	2711	0	0	0	0
24	2340.	0	0	0	0

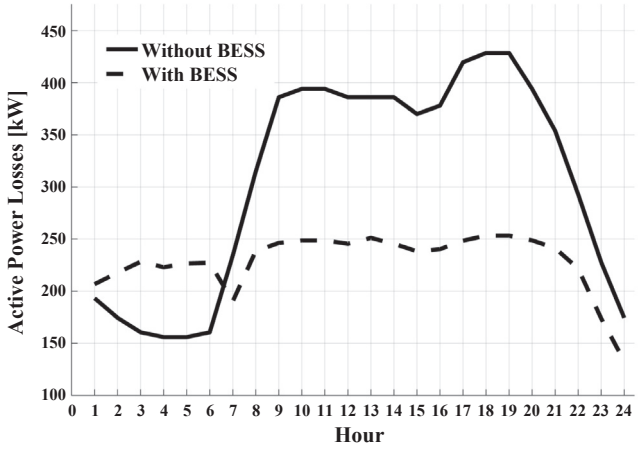

Fig. 7. Total hourly active power losses with and without BESS 1 and BESS 2.

in Fig. 7. As the figure demonstrates, using the BESS enhances losses in the off-peak periods but with a lower ratio than the peak periods. This results to 1853.728 kWh net reduction in the daily losses. Regarding the power losses nature, this reduction is a result of decreasing network reactive power flows besides load leveling.

Voltage magnitude of the network buses for the peak period (hours 18 and 19) is presented in Fig. 8. The reason for demonstrating voltages at this time period is that the highest voltage drops occurs here. Therefore, the effect of the BESS to compensate network voltages can be clarified easily. As in the figure, proper modeling and scheduling of the BESS reactive power tend to flatten the voltage profile. As it can be concluded from the results, the network is face with voltage drop at almost all time periods instead voltage increase and therefore it needs reactive power injection. Based on this fact, the reactive power absorption (charging) of the BESSs for all the time periods is zero while in the contrary they inject reactive power at all of the time periods. The reason is to rise voltage of the buses, dropped because of the long radial connecting feeders.

Fig. 9 shows the generated reactive power by each of the BESSs versus the reactive load of the buses. The reactive power supplied by both of the BESSs is almost equal and propositional to the

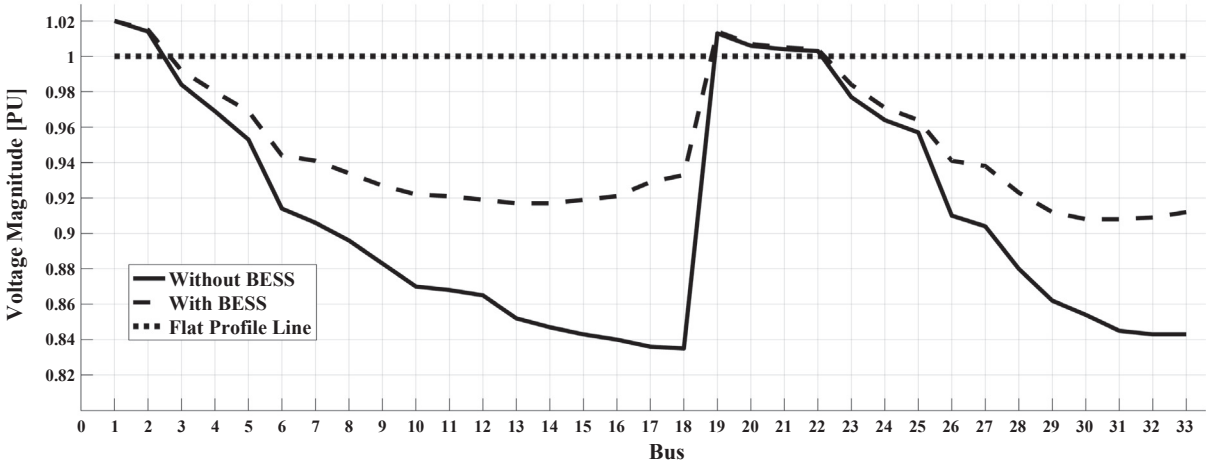

Fig. 8. Bus voltage magnitudes at peak hour with and without BESS 1 and BESS 2.

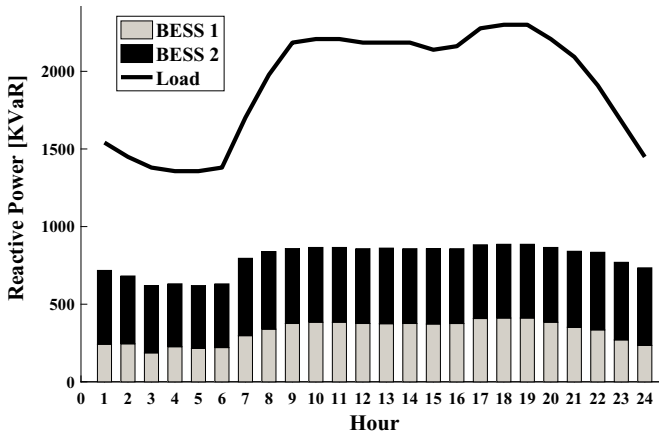

Fig. 9. Discharging reactive power of BESS 1 and BESS 2 along with the reactive load.

reactive power requirements of the network. Injecting reactive power by the BESSs have caused compensation of the reactive power demand and losses of the network which results to reduction of the reactive power output of the substation, in turn. This reduction will release capacity of the substation and give chance to contribute more in the active power requirements of the network without expansion plans. It should be noted that, as the simulation outputs proves, modeling and utilizing BESS reactive power in the network results in diminishing reactive power flows. This matter has a set of favorable consequences including:

- bus voltage improvement
- loss reduction
- more load leveling
- capacity release for both the substation and the feeders

4. Conclusions

In this paper a new model is proposed for BESS modeling and optimal daily scheduling in electric power distribution networks. Beside active power, reactive power contribution of the BESS is also modeled based on the capability curve. The proposed model benefits from linear structure which guarantees convergence to the global optimal and can be easily solved by using strong commercial solvers. The model is implemented on a test case under various scenarios. Although deploying the BESS in the network yields various benefit, modeling and scheduling of the BESS reactive power offers extra profits. Results of the simulations confirm that the proposed modeling and scheduling of the BESS will enhance its benefits as follow. The total daily operation cost is decreased by 3.7 percent with respect to the case in which the BESS reactive power contribution in not considered. In addition, voltage index of the buses is approximately improved by 30 percent which results to a flatter voltage profile. Moreover, total daily active and reactive power losses of the network demonstrate a 23.90 and 22.50 percent reduction, respectively. It can be concluded that the obtained extra benefits owing to considering the BESS reactive power can help to compensate high investment costs of the storage devices.

Appendix. Piecewise Linearization

The non-linear square functions appeared in the generation cost, BESS charging and discharging powers, and power flow voltage angle and magnitude are linearized by using piece-wise linearization technique. The method is described in the following. Figure a1 demonstrates the general idea of the method. Independent and dependent variables of the function are denoted by x and f(x), respectively. As in the figure, a non-linear function similar to f(x) can approximate by a set of linear functions. Each linear function is a straight line with constant slope.

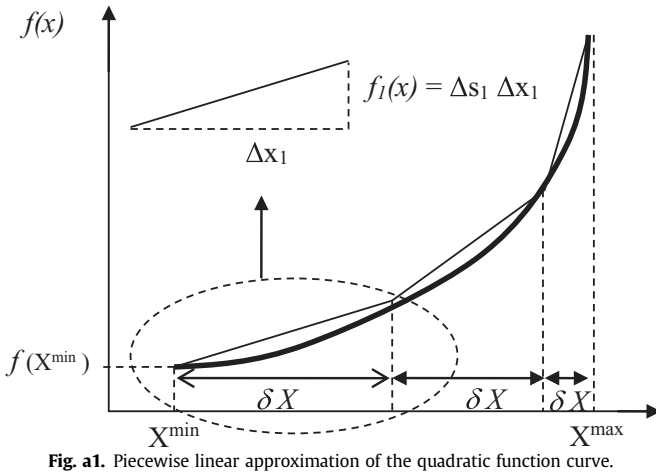

Fig. a1. Piecewise linear approximation of the quadratic function curve.

First step to linearize f(x) is defining number of the linearizing

blocks or straight lines. Increasing the number of straight lines will increase accuracy of the approximation in expense of run time. Equation (a1) shows that if XMin and XMax denote minimum and maximum bound of the x and R stands for desired number of linearizing blocks, then $\delta X$is width of each block. Length of each line segment (Δx_r) on the x axis is limited to the defined block sized, as in equation (a2). Slope of each line segment, denoted by Δs_r, can be easily calculated from (a3). for example, If the original non-linear function is a square function then slope of each line segment will be equal to (a.4). Then the original non-linear function can be approximated by its initial value (denoted by $f(X^{\min})$) in addition to the summation over all linear function, as (a1) demonstrates. Each linear function is equal to the line segment slope multiplied by the corresponding variable denoted by Δx_r . The line segments start from 1 and end with R. it should be noted that Δx_r is a positive variable and its summation over all segments will be equal to the original value of the x, as (a5) and (a6) show.

$$\delta X = \frac{X^{Max} - X^{Min}}{R} \tag{a1}$$

$$\Delta x_r \le \delta X \quad , \quad r \in \Omega_R \tag{a2}$$

$$\Delta s_r = \frac{f(x_r^{\max}) - f(x_r^{\min})}{\delta X} \tag{a3}$$

$$\Delta s_r = (2r-1)\delta X \tag{a4}$$

$$f(x) = f\left(X^{\min}\right) + \sum_{r=1}^{R} \Delta s_r \, \Delta x_r \tag{a5}$$

$$\Delta x_r \ge 0 \quad , \quad \forall \, r \in \Omega_R \tag{a6}$$

$$\sum_r \Delta x_r = x \tag{a7}$$

To ensure that line segments are filled up from the beginning, an additional equation is required. This situation is established in (a8) wherein Ir denotes a set of auxiliary binary variables. It should be noted that, if original non-linear function placed in a minimizing objective function, this equation is not required. Because, the minimization procedure automatically selects line segments from the beginning, for example generation cost function.

$$\delta X \, I_r \le \Delta x_r \le \delta X \, I_{r-1} \quad , \quad r \in \Omega_R \tag{a8}$$

Equations (a1) to (a8) are valid for a situation in which variable x takes only positive variables. Otherwise, some new equations are needed as shown. In this regard, (a7) should be replaced with (a9) and then (a7) to (a7) add to the problem. These new equations ensure that negative values of the x will be treated as positive values similar to the original non-linear function. In these equations, x+ and x - are auxiliary positive continuous variables and Bx is an auxiliary binary variable.

$$\sum_r \Delta x_r = x^+ - x^- \tag{a9}$$

$$x = x^+ - x^- \tag{a10}$$

$$x^+ \le B \, X^{Max} \tag{a11}$$

$$x^- \le (1 - Bx) \, X^{Max} \tag{a12}$$

$$x^+ \ge 0 \tag{a13}$$

$$x^- \ge 0 \tag{a14}$$

References

Awad, Ahmed SA., Tarek, HM El-Fouly, Salama, Magdy MA., 2014. Optimal ESS allocation and load shedding for improving distribution system reliability. IEEE Trans. Smart Grid 5 (5), 2339–2349.

Azizivahed, Ali, et al., 2018. A new bi-objective approach to energy management in distribution networks with energy storage systems. IEEE Trans. Sustain. Energy 9 (1), 56–64.

Baran, Mesut E., Wu, Felix F., 1989. Network reconfiguration in distribution systems for loss reduction and load balancing. IEEE Trans. Power Deliv. 4 (2), 1401–1407.

Bennett, Christopher J., Stewart, Rodney A., Lu, Jun Wei, 2015. Development of a three-phase battery energy storage scheduling and operation system for low voltage distribution networks. Appl. Energy 146, 122–134.

Brook, Anthony, Kendrick, David, Alexander, Meeraus, 1988. GAMS, a user's guide. ACM Signum Newslett. 23, 10–11, 3-4.

Cplex, I.L.O.G., 2007. 11.0 User's Manual. ILOG SA, Gentilly, France, p. 32.

Grigg, Cliff, et al., 1999. The IEEE reliability test system-1996. A report prepared by the reliability test system task force of the application of probability methods subcommittee. IEEE Trans. Power Syst. 14 (3), 1010–1020.

Grillo, Samuele, et al., 2012. Optimal management strategy of a battery-based storage system to improve renewable energy integration in distribution networks. IEEE Trans. Smart Grid 3 (2), 950–958.

Hemmati, Reza, Saboori, Hedayat, 2016. Short-term bulk energy storage system scheduling for load leveling in unit commitment: modeling, optimization, and sensitivity analysis. J. Adv. Res. 7 (3), 360–372.

Hemmati, Reza, Saboori, Hedayat, 2017. Stochastic optimal battery storage sizing and scheduling in home energy management systems equipped with solar photovoltaic panels. Energy Build. 152, 290–300.

Hemmati, Reza, Saboori, Hedayat, Ahmadi Jirdehi, Mehdi, 2017. Stochastic planning and scheduling of energy storage systems for congestion management in electric power systems including renewable energy resources. Energy 133, 380–387.

Hosseina, Majid, Taghi Bathaee, Seyed Mohammad, 2016. Optimal scheduling for distribution network with redox flow battery storage. Energy Convers. Manag. 121, 145–151.

Kleinberg, Michael, et al., 2014. Energy storage valuation under different storage forms and functions in transmission and distribution applications. Proc. IEEE 102 (7), 1073–1083.

Lawder, Matthew T., et al., 2014. Battery energy storage system (BESS) and battery management system (BMS) for grid-scale applications. Proc. IEEE 102 (6), 1014–1030.

Liu, Weijia, et al., 2016. Multi-objective restoration optimisation of power systems with battery energy storage systems. IET Gener., Transm. Distrib. 10 (7), 1749–1757.

Mahela, Om Prakash, Abdul, Gafoor Shaik, 2016. Power quality improvement in distribution network using DSTATCOM with battery energy storage system. Int. J. Electr. Power Energy Syst. 83, 229–240.

Pimm, Andrew J., Cockerill, Tim T., Taylor, Peter G., 2018. The potential for peak shaving on low voltage distribution networks using electricity storage. J. Energy Storage 16, 231–242.

Reihani, Ehsan, et al., 2016. Energy management at the distribution grid using a battery energy storage system (BESS). Int. J. Electr. Power Energy Syst. 77, 337–344.

Sabillon-Antunez, Carlos, et al., 2017. Volt-VAr control and energy storage device operation to improve the electric vehicle charging coordination in unbalanced distribution networks. IEEE Trans. Sustain. Energy 8 (4), 1560–1570.

Saboori, Hedayat, Abdi, Hamdi, 2013. Application of a grid scale energy storage system to reduce distribution network losses. In: Electrical Power Distribution Networks (EPDC), 2013 18th Conference on. IEEE.

Saboori, Hedayat, Hemmati, Reza, 2016. Optimal management and planning of storage systems based on particle swarm optimization technique. J. Renew. Sustain. Energy 8 (2), 024105.

Saboori, Hedayat, Hemmati, Reza, 2017. Maximizing DISCO profit in active distribution networks by optimal planning of energy storage systems and distributed generators. Renew. Sustain. Energy Rev. 71, 365–372.

Saboori, Hedayat, et al., 2017. Energy storage planning in electric power distribution networks–A state-of-the-art review. Renew. Sustain. Energy Rev. 79, 1108–1121.

Watson, Jeremy Donald, Watson, Neville R., Lestas, Ioannis, 2018. Optimized dispatch of energy storage systems in unbalanced distribution networks. IEEE Trans. Sustain. Energy 9 (2), 639–650.

Whittingham, M. Stanley, 2012. History, evolution, and future status of energy storage. In: Proceedings of the IEEE 100.Special Centennial Issue,

pp. 1518–1534.
Yang, Zhifang, et al., 2017. Solving OPF using linear approximations: fundamental analysis and numerical demonstration. IET Gener., Transm. Distrib. 11 (17), 4115–4125.
Yuan, Haoyu, et al., Jan 2018. Novel linearized power flow and linearized OPF models for active distribution networks with application in distribution LMP. IEEE Trans. Smart Grid 9 (1), 438–448.
Zhang, Hui, et al., 2013. An improved network model for transmission expansion planning considering reactive power and network losses. IEEE Trans. Power Syst. 28 (3), 3471–3479.
Zhang, Yongxi, et al., 2017. Optimal placement of battery energy storage in distribution networks considering conservation voltage reduction and stochastic load composition. IET Gener., Transm. Distrib. 11 (15), 3862–3870.